VNU Journal of Science: Mathematics - Physics

Journal homepage: https://js.vnu.edu.vn/MaP

Original Article

Order of Magnetic Transitions in $La(Fe_{1-x}Si_x)_{13}$ Induced by Random Anisotropy

Nguyen Tu Niem[1], Nguyen Thi Kim Oanh[2], Do Thi Kim Anh[1,*]

[1]*VNU University of Science, 334 Nguyen Trai, Thanh Xuan, Hanoi, Vietnam*

[2]*Electric Power University, 235 Hoang Quoc Viet, Hanoi, Vietnam*

Received 12th March 2026
Revised 20th April 2026; Accepted 5th May 2026

Abstract. The temperature dependence of the magnetic moment in $La(Fe_{1-x}Si_x)_{13}$ compounds reveals the presence of both first-order and second-order magnetic phase transitions. The nature of the transition is governed by variations in the Si concentration, which induce significant modifications in the Fe_I–Fe_{II} interactions between Fe atoms occupying two non-equivalent sites. These effects can be effectively modeled as a form of random anisotropy, the resulting behavior of which is accurately described within the framework of the Blume-Capel model. Monte Carlo simulations demonstrate that the evolution from a first-order to a second-order magnetic transition in $La(Fe_{1-x}Si_x)_{13}$ compounds can be consistently reproduced by maintaining a fixed anisotropy probability p while systematically reducing the corresponding anisotropy amplitude D, yielding good agreement with experimental trends.

Keywords: $La(Fe_{1-x}Si_x)_{13}$, Magnetic transition, Random anisotropy, Monte Carlo simulation.

1. Introduction

Over the past two decades, research on the room-temperature magnetocaloric effect (MCE) has expanded rapidly because of its high efficiency, reduced energy consumption, environmental compatibility, and strong potential for applications in magnetic refrigeration [1-4]. Among candidate materials for room-temperature magnetic refrigeration, $La(Fe_{1-x}Si_x)_{13}$ compounds, which crystallize in the cubic $NaZn_{13}$-type structure, contain the highest fraction of the transition metal per formula unit compared with other rare-earth transition-metal intermetallic compounds [5, 6]. These compounds exhibit a giant MCE, which is further enhanced when it is associated with a first-order magnetic

* Corresponding author.
E-mail address: kimanh72@gmail.com

https//doi.org/10.25073/2588-1124/vnumap.5134

transition (FOMT) in the temperature dependence of the magnetic moment [1, 7-9]. The FOMT is generally attributed to competing Fe–Fe exchange interactions: antiferromagnetic (AFM) coupling occurs when the Fe–Fe interatomic distance is smaller than approximately 2.45 Å whereas ferromagnetic (FM) coupling emerges at larger separations [7-10]. However, theoretical approaches based solely on this mechanism, most commonly employing mean-field theory combined with a Brillouin function, have been unable to adequately reproduce the FOMT behavior in the vicinity of the critical temperature T_c [8, 9, 11].

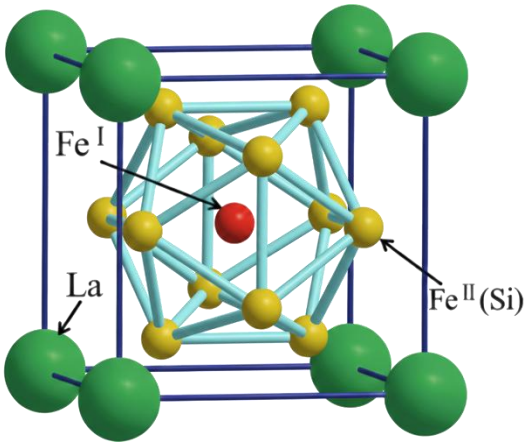

Figure 1. Crystal structure of the $La(Fe_{1-x}Si_x)_{13}$ compounds adopting the cubic $NaZn_{13}$-type structure, characterized by the space group *Fm*3*c* [7].

The crystal structure of the $La(Fe_{1-x}Si_x)_{13}$ compounds is illustrated in Fig. 1. Within the cubic framework formed by La atoms at the 8*a* site, the Fe_I atom at the 8*b* site is surrounded by an icosahedron composed of 12 Fe_{II} atoms occupying the 96*i* site, where Si substitution preferentially occurs. Because both La and Si are nonmagnetic, the dominant magnetic contribution arises from the icosahedral cluster $(Fe_I–Fe_{II})_{13}$, which can be regarded as a magnetic superatom embedded in the cubic lattice. According to Refs. [8, 9], increasing the Si concentration does not significantly modify the $(Fe_{II}–Fe_{II})$ interatomic distance (approximately 2.53 Å), thereby preserving a stable FM coupling among Fe_{II} atoms. In contrast, Si substitution primarily affects the $(Fe_I–Fe_{II})$ distance. The FOMT is observed when the average $(Fe_I–Fe_{II})$ separation approaches approximately 2.45 Å. Under this condition, FM and AFM exchange interactions coexist within each $(Fe_I–Fe_{II})_{13}$ superatom, allowing spin-up and spin-down moments to coexist within a single superatom. As a result, the oppositely oriented spins may partially compensate one another, thereby reducing the net magnetic moment of the superatom. Consequently, each $(Fe_I–Fe_{II})_{13}$ superatom can be modeled as a multistate spin located at the vertices of the cubic lattice. Within this framework, the overall $(Fe_I–Fe_{II})$ exchange interactions inside a superatom are treated as an effective random anisotropy, arising from the random spatial distribution of Si atoms and governing the magnitude of the corresponding multistate spin. Furthermore, owing to the predominance of Fe_{II} atoms at the surface of the superatom, the interaction between neighboring multistate spins can be reasonably approximated as a uniform FM exchange coupling.

Since the total spins in $La(Fe_{1-x}Si_x)_{13}$ compounds can be readily aligned by a weak external field [12], their magnetic behavior is reasonably described within an Ising-like framework. In this context, the Blume-Capel (BC) model with random anisotropy, as the simplest model capable of exhibiting the FOMT, emerges as a suitable candidate [13, 14]. Recent investigations of this model have successfully reproduced the FOMT characteristics observed in the single-crystal $Cr_{11}Ge_{19}$ [15] and in doped

perovskite manganite oxides $AMnO_3$ [16] by utilizing advanced Monte Carlo (MC) techniques that overcome the limitations of conventional mean-field approaches.

In this study, MC simulations are performed and show good agreement with the experimental data on the magnetic transition in $La(Fe_{1-x}Si_x)_{13}$ compounds reported in Ref. [12]. This consistency supports the validity of the model and highlights the important role of random anisotropy in governing the magnetic transition mechanism.

2. Model and Monte Carlo Simulation

2.1. Blume-Capel Model

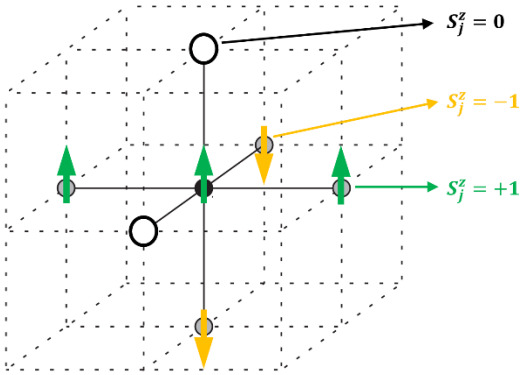

Figure 2. Representation of the cubic spin lattice structure adopted for the spin-1 Blume-Capel model.

To elucidate the variation in magnetic transition types observed in the $La(Fe_{1-x}Si_x)_{13}$ compounds, a cubic lattice of size $N = L \times L \times L$ with periodic boundary conditions applied along all spatial directions is simulated within the framework of the spin-1 BC model incorporating random anisotropy (Fig. 2). The Hamiltonian of the system is expressed as follows:

$$H_{BC} = -J \sum_{\langle i,j \rangle} S_i^z S_j^z + \sum_j D_j \left(S_j^z\right)^2 - h \sum_j S_j^z \quad (1)$$

Here, the variable S_i^z, which can take the discrete values ±1 or 0, denotes the z-component of a classical spin $S = 1$ located at lattice site i. The first summation is performed over all nearest neighbor pairs $\langle i,j \rangle$, where a positive exchange interaction $J > 0$ favors ferromagnetic alignment between adjacent spins. The final term represents the contribution of an external magnetic field of strength h. In addition, the site-dependent random anisotropy field D_j is introduced in the second term, which obeys a bimodal probability distribution [15-20],

$$P(D_j) = p\delta(D_j - D) + (1 - p)\delta(D_j) \quad (2)$$

In this formulation, the anisotropic field at each lattice site takes a finite value D with probability p, while it becomes zero with probability $1\text{-}p$. For the numerical analysis, the dimensionless temperature T is defined in units of J/k_B. Accordingly, it can be related to the experimental temperature τ, expressed in Kelvin, through the relation $T = k_B\tau/J$. The dimensionless magnetic moment per spin is evaluated as

$$m = \frac{\left\langle \sum_{i=1}^{N} S_i^z \right\rangle}{N} \quad (3)$$

2.2. Monte Carlo Simulation

MC simulations are performed on a cubic lattice with linear size $L = 16$, which is sufficient to determine the physical properties according to Ref. [21]. The calculations follow a two-stage computational scheme.

In the first stage, the approximate transition temperature T_c is determined by applying the standard Metropolis algorithm [22] combined with a simulated annealing procedure, during which the system is progressively cooled from a high-temperature configuration. At each temperature, 10^5 MC sweeps are executed to ensure thermal equilibration. Subsequently, an additional 10^5 sweeps are carried out to evaluate the thermal average of the dimensionless magnetic moment.

In the second stage, the parallel tempering method, also known as replica exchange MC [23], is implemented over a set of temperatures distributed symmetrically around the previously estimated T_c [24]. The replicas corresponding to these temperatures are simulated simultaneously, and 10^4 exchange attempts between adjacent replicas are proposed. Each exchange attempt is separated by 100 Metropolis sweeps. The statistical averages of the dimensionless magnetic moment are subsequently evaluated from the accumulated simulation data.

3. Results and Discussion

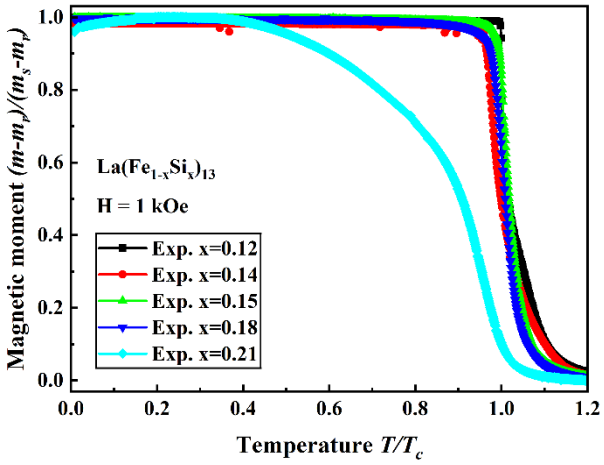

Figure 3. The normalized magnetic moment $(m-m_r)/(m_s-m_r)$ as a function of the normalized temperature T/T_c for the experimental results of $La(Fe_{1-x}Si_x)_{13}$ [12].

According to Fig. 3 in Ref. [12], no systematic correlation is observed between increasing Si content in $La(Fe_{1-x}Si_x)_{13}$ and either the saturation or the remanent magnetic moment. This behavior originates from the itinerant-electron nature of magnetism in $La(Fe_{1-x}Si_x)_{13}$ [6, 25-28], where magnetic ordering is governed by the splitting between spin-up and spin-down subbands in the electronic density of states rather than by localized magnetic moments [29, 30].

To clearly examine the magnetic transition behavior (FOMT and SOMT) and eliminate the influence of itinerant-electron magnetism, which cannot be fully described by localized-magnetic-moment models such as the BC model, we analyze the temperature dependence of the magnetic moment in $La(Fe_{1-x}Si_x)_{13}$ using a normalized representation that removes the effects of different saturation and remanent magnetic moments. The experimental thermomagnetic curves reported in Ref. [12] are replotted in Fig. 3 in relative units, where m_r denotes the remanent magnetic moment, m_s the saturation magnetic moment,

and T_c the critical temperature. As shown in Fig. 3, $La(Fe_{1-x}Si_x)_{13}$ exhibits a SOMT at $x = 0.21$, whereas a FOMT is observed for compositions in the range $x = 0.12$ - 0.18. Although the FOMT behavior is nearly identical for $x = 0.12$ - 0.18, the composition $x = 0.18$ displays the sharpest change at the critical temperature, which is most consistent with the definition of a FOMT in phase transition theory [31].

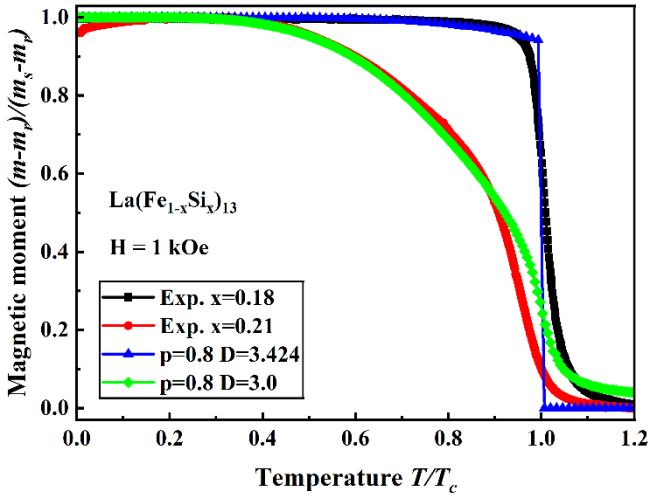

Figure 4. Comparison between experimental results and MC simulations for the normalized magnetic moment $(m\text{-}m_r)/(m_s\text{-}m_r)$ as a function of normalized temperature (T/T_c).

In Fig. 4, the normalized temperature (T/T_c) dependence of the normalized magnetic moment $(m - m_r)/(m_s - m_r)$ for $La(Fe_{1-x}Si_x)_{13}$ compounds under low-field cooling at $H = 1$ kOe is fitted to the spin-1 BC model with a fixed external field $h \approx 4 \times 10^{-4}$, anisotropy probability $p = 0.8$, and varying anisotropy amplitude D. Qualitatively, the FOMT behavior for the composition $x = 0.18$ is well reproduced by MC simulations of the spin-1 BC model with parameters $p = 0.8$, $D = 3.424$, and $h \approx 4\times10^{-4}$. Similarly, the SOMT behavior for $x = 0.21$ is consistent with MC results obtained using $p = 0.8$, $D = 3.0$, and $h \approx 4\times10^{-4}$. A slight deviation near the critical temperature between experimental observations and MC results in both the FOMT and SOMT cases may arise from the contribution of itinerant 3*d* electrons, finite-size effects in the MC simulations, or the multi-state spin nature of the $(Fe_I\text{-}Fe_{II})_{13}$ superatom, for which a spin-1 description may be insufficient.

For the FOMT composition $x = 0.18$, with an experimental critical temperature $\tau_c \approx 251$ K corresponding to a dimensionless critical temperature $T_c \approx 0.77$ for $p = 0.8$ and $D = 3.424$, the exchange interaction is estimated as $J = k_B\tau_c/T_c \approx 28$ meV. Using this exchange energy scale, the relationship between the experimental external field H and the simulation field h is given by $H = hJ/(g\mu_B)$, where the Landé factor is $g \approx 2$ and μ_B denotes the Bohr magneton. Accordingly, the experimental field $H = 1$ kOe corresponds to a simulation field $h \approx 4\times10^{-4}$, which is applied consistently in all MC simulations.

The random-anisotropy-driven FOMT-to-SOMT transformation in $La(Fe_{1-x}Si_x)_{13}$ can be interpreted as follows. Because the change in Si substitution between $x = 0.18$ and $x = 0.21$ is relatively small, we assume that this compositional variation has a negligible effect on the anisotropy probability $p = 0.8$, while primarily modifying the anisotropy strength D. For $x = 0.18$, where the average Fe_I–Fe_{II} distance is approximately 2.45 Å, AFM and FM interactions within each $(Fe_I\text{–}Fe_{II})_{13}$ superatom are comparable in magnitude. As a result, neither interaction dominates, allowing both spin-up and spin-down moments to coexist within each superatom. Partial cancellation between these oppositely aligned spins suppresses the net magnetic moment of the superatom. Within the BC framework, this situation can be effectively

represented by a relatively large anisotropy amplitude, $D = 3.424$. For $x = 0.21$, the increased Si content enlarges the Fe_I–Fe_{II} distance and effectively converts most AFM couplings into FM ones. As a consequence, the occurrence of suppressed-magnetic-moment states is significantly reduced. Within the BC description, this behavior corresponds to a smaller anisotropy amplitude, $D = 3.0$, thereby accounting for the transition from FOMT to SOMT.

In addition, the MC results for the temperature dependence of the magnetic moment at $h \approx 4 \times 10^{-4}$, $p = 0.8$, and various values of D are presented in Fig. 5. These results further support the correlation between increasing Si content and the reduction of the anisotropy strength D at fixed probability p, as reflected by the corresponding increase in the critical temperature T_c. As shown in Fig. 5, for $p = 0.8$, the tricritical point separating FOMT and SOMT occurs at $D_c \approx 3.4$. This critical value is expected to correspond to the compositional range $0.18<x<0.21$ in the $La(Fe_{1-x}Si_x)_{13}$ compounds.

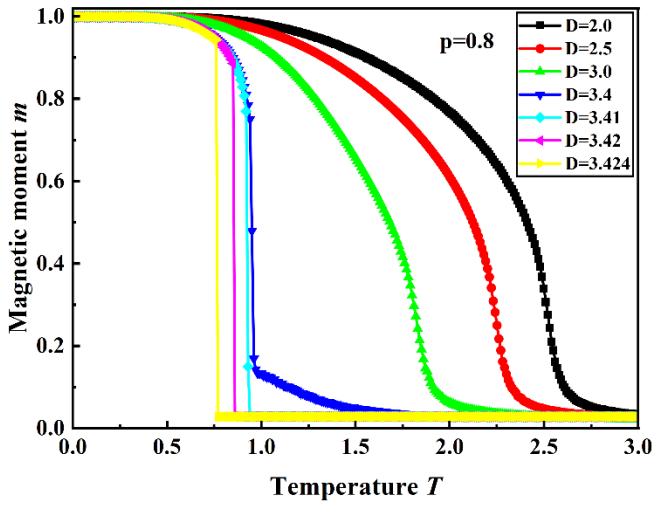

Figure 5. MC simulation results for the temperature dependence of the magnetic moment at a fixed external field $h \approx 4 \times 10^{-4}$ and anisotropy probability $p = 0.8$, for various anisotropy strengths D.

4. Conclusion

Within the theoretical framework, the influence of Si substitution in $La(Fe_{1-x}Si_x)_{13}$ compounds can be mapped onto a random-anisotropy scenario within the spin-1 BC model. The MC calculations successfully reproduce the experimentally observed crossover from FOMT to SOMT by keeping the anisotropy probability fixed at $p = 0.8$ and progressively decreasing the anisotropy amplitude D. Specifically, the FOMT observed for $x = 0.18$ corresponds to $D = 3.424$ with $h \approx 4 \times 10^{-4}$, whereas the SOMT at $x = 0.21$ is described by a lower anisotropy strength, $D = 3.0$, under identical p and h.

For $p = 0.8$, the larger anisotropy amplitude $D = 3.424$, associated with the FOMT, corresponds to an average Fe_I–Fe_{II} distance of approximately 2.45 Å. In contrast, the smaller anisotropy amplitude $D = 3.0$, associated with the SOMT, corresponds to an average Fe_I–Fe_{II} distance greater than 2.45 Å. Moreover, for $p = 0.8$, the critical anisotropy separating FOMT and SOMT is found at $D_c \approx 3.4$, which aligns with the experimental compositional interval $0.18<x<0.21$ where the transition order changes.

Acknowledgment

This research was funded by the research project QG.25.23 of Vietnam National University, Hanoi. We also thank Phong H. Nguyen and Prof. Cong T. Bach (VNU University of Science) for valuable discussions.

Declaration of Generative AI and AI-assisted Technologies in the Writing Process

During the preparation of this work we used ChatGPT in order to check grammars. After using this tool/service, we reviewed and edited the content as needed and take full responsibility for the content of the publication.

References

[1] A. Vinod, D. A. Babu, M. Wuppulluri, A Short Review on the Evolution of Magnetocaloric $La(Fe,Si)_{13}$ and Its Fabrication Through Melt Spinning, ACS Omega, Vol. 9, 2024, pp. 11110-11128, https://doi.org/10.1021/acsomega.3c08622.

[2] T. J. D. Rose, R. K. Chouhan, A. Doyle, A. K. Pathak, Y. Mudryk, LaFeSi–$LaFe_{13-x}Si_x$ Composites: Modulating Magnetic and Magnetocaloric Properties Through Inherent Stress Manipulation, Journal of Applied Physics, Vol. 136, 2024, pp. 035101, https://doi.org/10.1063/5.0212650.

[3] K. Imaizumi, A. Fujita, A. Suzuki, M. Kobashi, K. Ozaki, Improvement of Magnetocaloric Effect in $La(Fe_xSi_{1-x})_{13}$ by Dealing With Inhibitory Microstructures at High Fe Concentration, Acta Materialia, Vol. 227, 2022, pp. 117726, https://doi.org/10.1016/j.actamat.2022.117726.

[4] K. Imaizumi, A. Fujita, A. Suzuki, M. Kobashi, K. Ozaki, Microstructure and Magnetocaloric Property of Homogeneous $La(Fe_xSi_{1-x})_{13}$ Compounds Fabricated by Laser Fusion Using a Powder Mixture of Fe and La–Si Compounds, Journal of Alloys and Compounds, Vol. 901, 2022, pp. 163706, https://doi.org/10.1016/j.jallcom.2022.163706.

[5] P. I. Kripyakevich, O. S. Zarechnyuk, E. I. Gladyshevsky, O. I. Bodak, Crystal Structure of Compounds With the $NaZn_{13}$ Type, Zeitschrift für Anorganische Chemie, Vol. 358, 1968, pp. 90, https://doi.org/10.1002/zaac.19683580110.

[6] T. T. M. Palstra, J. A. Mydosh, G. J. Nieuwenhuys, A. M. van der Kraan, K. H. J. Buschow, Critical Behaviour of Magnetization and Electrical Resistivity in Cubic $La(Fe,Si)_{13}$ Compounds, Journal of Magnetism and Magnetic Materials, Vol. 36, 1983, pp. 290, https://doi.org/10.1016/0304-8853(83)90128-2.

[7] W. Wang, R. Huang, W. Li, J. Tan, Y. Zhao, S. Li, C. Huang, L. Li, Zero Thermal Expansion in $NaZn_{13}$-Type $La(Fe,Si)_{13}$ Compounds, Physical Chemistry Chemical Physics, Vol. 17, 2015, pp. 2352-2356, https://doi.org/10.1039/C4CP04672B.

[8] G. J. Wang, F. Wang, N. L. Di, B. G. Shen, Z. H. Cheng, Hyperfine Interactions and Band Structures of $LaFe_{13-x}Si_x$ Intermetallic Compounds with Large Magnetic Entropy Changes, Journal of Magnetism and Magnetic Materials, Vol. 303, No. 1, 2006, pp. 84-91, https://doi.org/10.1016/j.jmmm.2005.10.231.

[9] X. B. Liu, Z. Altounian, D. H. Ryan, Structure and Magnetic Transition of $LaFe_{13-x}Si_x$ Compounds, Journal of Physics: Condensed Matter, Vol. 15, 2003, pp. 7385, https://doi.org/10.1088/0953-8984/15/43/020.

[10] D. Givord, R. Lemaire, Magnetic Transition and Anomalous Thermal Expansion in R_2Fe_{17} Compounds, IEEE Transactions on Magnetics, Vol. 10, No. 2, 1974, pp. 109-113, https://doi.org/10.1109/TMAG.1974.1058311.

[11] L. M. M. Ramírez, J. Y. Law, J. M. Borrego, A. Barcza, J. M. Greneche, V. Franco, First-Order Phase Transition in High-Performance $La(Fe,Mn,Si)_{13}H$ Despite Negligible Hysteresis, Journal of Alloys and Compounds, Vol. 950, 2023, pp. 169883, https://doi.org/10.1016/j.jallcom.2023.169883.

[12] D. T. K. Anh, V. V. Hiep, Samples Preparation, Structure and Magnetic Properties of $La(Fe_{1-x}Si_x)_{13}$ Compounds, VNU Journal of Science: Mathematics and Physics, Vol. 28, 2012, pp. 1-5, https://doi.org/10.25073/2588-1124/vnumap.4353.

[13] M. Blume, Theory of the First-Order Magnetic Phase Change in UO_2, Physical Review, Vol. 141, 1966, pp. 517-524, https://doi.org/10.1103/PhysRev.141.517.

[14] H. W. Capel, On the Possibility of First-Order Phase Transitions in Ising Systems of Triplet Ions with Zero-Field Splitting, Physica, Vol. 32, No. 5, 1966, pp. 966-988, https://doi.org/10.1016/0031-8914(66)90027-9.

[15] P. H. Nguyen, N. T. Nguyen, H. D. Nguyen, H. T. L. Nguyen, C. T. Bach, G. H. Bach, Random-Anisotropy Driven Giant Magnetic Entropy Change in First-Order Magnetic Transition Under External Fields, Journal of Alloys and Compounds, Vol. 1017, 2025, pp. 179001, https://doi.org/10.1016/j.jallcom.2025.179001.

[16] P. H. Nguyen, G. H. Bach, Thermodynamic Properties of the First-Order Magnetic Transition in the Highly Anisotropic 2D Blume–Capel Model, Communications in Physics, Vol. 35, No. 3, 2025, pp. 203-212, https://doi.org/10.15625/0868-3166/22722.

[17] G. H. Bach, O. K. T. Nguyen, C. V. Nguyen, C. T. Bach, First-Order Magnetization Process in Polycrystalline Perovskite Manganite, Materials Transactions, Vol. 56, No. 9, 2015, pp. 1320-1322, https://doi.org/10.2320/matertrans.MA201507.

[18] O. K. T. Nguyen, P. H. Nguyen, L. D. Dang, C. T. Bach, G. H. Bach, Fluctuation Inducing Fractional Magnetization Behavior on the Shastry–Sutherland Lattice, Physica B: Condensed Matter, Vol. 583, 2020, pp. 412012, https://doi.org/10.1016/j.physb.2020.412012.

[19] O. K. T. Nguyen, P. H. Nguyen, N. T. Nguyen, C. T. Bach, H. D. Nguyen, G. H. Bach, Monte Carlo Investigation for an Ising Model with Competitive Magnetic Interactions in the Dominant Ferromagnetic-Interaction Regime, Communications in Physics, Vol. 33, 2023, pp. 205, https://doi.org/10.15625/0868-3166/18109.

[20] P. H. Nguyen, Q. M. Le, O. K. T. Nguyen, C. T. Bach, G. H. Bach, Effective Field Theory Investigation for a Disordered Ising Model in the Description of Amorphous Magnetic Systems, Journal of Non-Crystalline Solids, Vol. 643, 2024, pp. 123165, https://doi.org/10.1016/j.jnoncrysol.2024.123165.

[21] I. Puha, H. T. Diep, Random-Bond and Random-Anisotropy Effects in the Phase Diagram of the Blume–Capel Model, Journal of Magnetism and Magnetic Materials, Vol. 224, No. 1, 2001, pp. 85-92, https://doi.org/10.1016/S0304-8853(00)01378-0.

[22] N. Metropolis, A. W. Rosenbluth, M. N. Rosenbluth, A. H. Teller, E. Teller, Equation of State Calculations by Fast Computing Machines, The Journal of Chemical Physics, Vol. 21, 1953, pp. 1087-1092, https://doi.org/10.1063/1.1699114.

[23] K. Hukushima, K. Nemoto, Exchange Monte Carlo Method and Application to Spin Glass Simulations, Journal of the Physical Society of Japan, Vol. 65, No. 6, 1996, pp. 1604-1608, https://doi.org/10.1143/JPSJ.65.1604.

[24] P. H. Nguyen, C. T. Bach, H. D. Nguyen, H. T. L. Nguyen, H. H. Mai, D. Q. Dao, G. H. Bach, Field-Driven Magnetization Processes, Magnetocaloric Effect and Tunneling Magnetoconductivity in Bilayer CrI_3 Thin Films: Insights From Replica-Exchange Monte Carlo Simulations, Acta Materialia, Vol. 307, 2026, pp. 121975, https://doi.org/10.1016/j.actamat.2026.121975.

[25] T. T. M. Palstra, G. J. Nieuwenhuys, J. A. Mydosh, K. H. J. Buschow, Magnetic Properties of Cubic $La(Fe,Al)_{13}$ Intermetallic Compounds, Journal of Applied Physics, Vol. 55, 1984, pp. 2367, https://doi.org/10.1063/1.333667.

[26] T. T. M. Palstra, G. J. Nieuwenhuys, J. A. Mydosh, K. H. J. Buschow, Mictomagnetic, Ferromagnetic, and Antiferromagnetic Transitions in $La(Fe,Al)_{13}$, Physical Review B, Vol. 31, 1985, pp. 4622, https://doi.org/10.1103/PhysRevB.31.4622.

[27] A. Fujita, K. Fukamichi, Giant Volume Magnetostriction Due to the Itinerant-Electron Metamagnetic Transition in $La(Fe,Si)_{13}$, IEEE Transactions on Magnetics, Vol. 35, 1999, pp. 1796, https://doi.org/10.1109/INTMAG.1999.837942.

[28] H. Yamada, K. Fukamichi, T. Goto, Itinerant-Electron Metamagnetism and Pressure Dependence of the Curie Temperature in $La(Fe,Si)_{13}$, Physical Review B, Vol. 65, 2002, pp. 024413, https://doi.org/10.1103/PhysRevB.65.024413.

[29] E. C. Stoner, Collective Electron Ferromagnetism, Proceedings of the Royal Society A, Vol. 165, 1938, pp. 372-414, https://doi.org/10.1098/rspa.1938.0066.

[30] K. H. J. Buschow, F. R. de Boer, Physics of Magnetism and Magnetic Materials, Springer, USA, 2003, https://doi.org/10.1007/b100503.

[31] H. Nishimori, G. Ortiz, Elements of Phase Transitions and Critical Phenomena, Oxford University Press, Oxford, 2011, https://doi.org/10.1093/acprof:oso/9780199577224.001.0001.